Cancer Cell
Article

Inactivation of Myocardin and p16 during Malignant Transformation Contributes to a Differentiation Defect

Michael Milyavsky,[1,5] Igor Shats,[1,5] Alina Cholostoy,[1] Ran Brosh,[1] Yosef Buganim,[1] Lilach Weisz,[1] Ira Kogan,[1] Merav Cohen,[1] Maria Shatz,[2] Shalom Madar,[1] Eyal Kalo,[1] Naomi Goldfinger,[1] Jun Yuan,[3] Shulamit Ron,[4] Karen MacKenzie,[3] Amir Eden,[4] and Varda Rotter[1,*]
[1] Department of Molecular Cell Biology
[2] Department of Biological Regulation
Weizmann Institute of Science, Rehovot 76100, Israel
[3] Children's Cancer Institute for Medical Research, Randwick, New South Wales 2031, Australia
[4] Institute of Life Sciences, The Hebrew University, Jerusalem 91904, Israel
[5] These authors contributed equally to this work.
*Correspondence: varda.rotter@weizmann.ac.il
DOI 10.1016/j.ccr.2006.11.022

SUMMARY

Myocardin is known as an important transcriptional regulator in smooth and cardiac muscle development. Here we found that myocardin is frequently repressed during human malignant transformation, contributing to a differentiation defect. We demonstrate that myocardin is a transcriptional target of TGFβ required for TGFβ-mediated differentiation of human fibroblasts. Serum deprivation, intact contact inhibition response, and the $p16^{ink4a}$/Rb pathway contribute to myocardin induction and differentiation. Restoration of myocardin expression in sarcoma cells results in differentiation and inhibition of malignant growth, whereas inactivation of myocardin in normal fibroblasts increases their proliferative potential. Myocardin expression is reduced in multiple types of human tumors. Collectively, our results demonstrate that myocardin is an important suppressive modifier of the malignant transformation process.

INTRODUCTION

Escape from the tissue/lineage-specific differentiation program is one of the fundamental aspects of tumorigenesis in general and sarcomagenesis in particular.

Human primary fibroblasts, which could be induced to undergo differentiation toward myofibroblasts and to some extent to smooth muscle cells (SMCs), might serve as a faithful model to study molecular mechanisms underlying differentiation defects in sarcomas and in the tumor stroma compartment, in which fibroblasts play an important role. The highly organized actin cytoskeleton of these cells is characterized by varying levels of smooth muscle α-actin (αSMA), smooth muscle myosin heavy chain (SM MHC), calponin (CNN1), and transgelin (SM22). The genes encoding these proteins are coordinately regulated at the transcriptional level in myofibroblasts and SMCs and therefore are informative indicators of the differentiation in these cell types (Kumar and Owens, 2003; Pipes et al., 2006). On the other hand, actin cytoskeleton undergoes transformation-associated disruption in fibroblasts. The molecular basis responsible for this differentiation disruption remains unclear (Button et al., 1995; Leavitt et al., 1985).

The most common oncogenic changes described in sarcomas include inactivation of $p16^{INK4A}$ (p16), *Rb1*, and *p53* tumor-suppressor genes (Helman and Meltzer,

SIGNIFICANCE

The malignant transformation process is associated with defects in cell-cycle regulation and disruption of the normal differentiation programs in both neoplastic and adjacent stroma cells. However, deregulation of the complex interplay between differentiation stimuli, mesenchymal tissue-specific transcription factors, and cell-cycle-regulatory machinery is not completely understood. In this study we identified a role in human carcinogenesis for the important regulator of cardiac and smooth muscle differentiation myocardin. We show that myocardin mRNA levels and activity are positively regulated by the p16/Rb pathway, providing a molecular link between cell-cycle and differentiation defects during tumor development. The antiproliferative activity of myocardin shown here suggests that its reactivation may represent an effective therapeutic approach in cancer treatment.

2003), which control progression through the cell cycle as a function of mitogen availability, contact inhibition, and oncogene activation. For some in vitro differentiation models, interference with intact cell-cycle regulation impairs subsequent differentiation. In some experimental settings where exit from the cell cycle is not required, maximal expression of differentiation markers is still dependent on the function of an intact Rb tumor-suppressor pathway (Halevy et al., 1995; Novitch et al., 1996).

Transforming growth factor β (TGFβ) is a potent regulator of differentiation in many tissues, including mesenchyme (Massague et al., 2000). Furthermore, TGFβ is involved in inflammation, fibrosis, and malignant transformation processes, in which fibroblasts, myofibroblasts, and SMCs play a pivotal role. Treatment of primary human fibroblasts with TGFβ results in the induction of the fibroblast-myofibroblast differentiation program (Chambers et al., 2003; Serini and Gabbiani, 1999).

Recently, it was found that myocardin (Myocd), a smooth and cardiac muscle-specific transcriptional regulator, is an essential transcriptional cofactor for a variety of SMC-specific genes (Wang et al., 2001). Myocardin drives transcription through interaction with the ubiquitous transcription factor serum response factor (SRF), which acts on a responsive element (CArG box) that is commonly found in many smooth muscle and myofibroblast gene promoters (Pipes et al., 2006). However, despite the established executive function of myocardin in SMC differentiation, its role in transformation and TGFβ-mediated myofibroblast differentiation is largely unknown.

The regulation of cytoskeletal/differentiation genes clearly involves a complex interplay between differentiation stimuli, mesenchymal tissue-specific transcription factors, and cell-cycle-regulatory machinery (Kumar and Owens, 2003). Oncogenic mutations may impinge on several levels of regulation along the differentiation process. Therefore, a detailed examination of the loss of cytoskeletal/differentiation markers in the context of controlled stepwise malignant transformation will provide insight to the molecular interactions between these two processes.

In our previous study, we found that hTERT-induced immortalization of WI-38 human fibroblasts (WI-38T) resulted in the spontaneous emergence of rapidly proliferating variants (T^{fast}). These clones had a defective response to contact inhibition and did not express the p16 tumor-suppressor gene (Milyavsky et al., 2003). Utilizing genome-wide expression profiling, we found that T^{fast} cells and their derivatives were characterized by a reduced expression of genes involved in various aspects of mesenchymal cell development and differentiation compared with primary WI-38 or early passage WI-38/hTERT cells (T^{slow}). Numerous genes that were downregulated encode well-characterized, functional markers of the myofibroblast phenotype αSMA, CALD1, SM-MHC, SM22, and CNN1 (Milyavsky et al., 2005).

In the present study, we found that human mesenchymal transformation is associated with a differentiation block accompanied by downregulation of myocardin in vitro and in vivo. We demonstrate that myocardin is positively regulated by the p16/Rb pathway. Moreover, myocardin is induced by TGFβ and is essential for TGFβ-induced myofibroblast differentiation. Ectopic expression of myocardin in tumor cells restores expression of differentiation markers and inhibits the transformed phenotype. Our results provide considerable insight into the regulation of myocardin and suggest that its downregulation is important for cancer development.

RESULTS

Human Mesenchymal Cells with Inactivated p16 Exhibit Disrupted Basal and TGFβ-Induced Myofibroblast Differentiation

Coordinated reduction in the expression of numerous differentiation markers observed in T^{fast} cells indicated that the cells acquired a defect in the fibroblast-myofibroblast differentiation program during immortalization (Milyavsky et al., 2005). To characterize this defect in detail, T^{slow} and T^{fast} WI-38 cells were treated with an inducer of myofibroblast differentiation, TGFβ, and analyzed for the induction of several differentiation markers by quantitative real-time PCR (QRT-PCR). These experiments were performed with confluent cultures in serum-free conditions, as is common practice in differentiation studies. In agreement with our previous findings, T^{fast} cells expressed barely detectable basal levels of p16 and reduced levels of several well-known myofibroblast markers, such as CNN1, αSMA, and SM-MHC compared with T^{slow} cells. Upon TGFβ treatment, a robust induction of these markers was evident in T^{slow} cells, but not in T^{fast} cells (Figure 1A), demonstrating a complete block in the TGFβ-induced myofibroblast differentiation program in T^{fast} cells. p16 levels were not affected by the TGFβ treatment in both T^{slow} and T^{fast} cells. Induction of immediate-early targets of TGFβ, such as JunB and Id1, was comparable in T^{slow} and T^{fast} cells, while the induction of $p15^{INK4B}$ growth inhibitor was blunted in T^{fast} cells (Figure 1B).

To substantiate the correlation between loss of p16 and deregulation of myofibroblast markers, additional strains of human mesenchymal cells were analyzed. To that end, early and late passages (psg 17 and psg 66, respectively) of the hTERT-immortalized human prostate-derived SMCs PM151T (Kogan et al., 2006) and precrisis and postcrisis premalignant MRC5T human fibroblasts (Taylor et al., 2004) were used. Both cell types exhibited downregulation of p16 during hTERT-mediated immortalization. In agreement with our observations in WI-38T cells, both immortalized mesenchymal strains had significantly lower basal levels of αSMA, SM22, and CNN1. In addition, postcrisis MRC5T cells exhibited reduced TGFβ-mediated myofibroblast differentiation (Figures 1C and 1D).

In an attempt to understand the molecular details underlying the differential TGFβ response in WI-38 T^{slow} and T^{fast} cells, we monitored the activation and levels of some classic components of the TGFβ pathway, such as SMAD2/3 and ERK1/2, under conditions identical to those used for the differentiation induction. Beyond subtle kinetic differences, p16-deficient WI-38 T^{fast} fibroblasts initiated

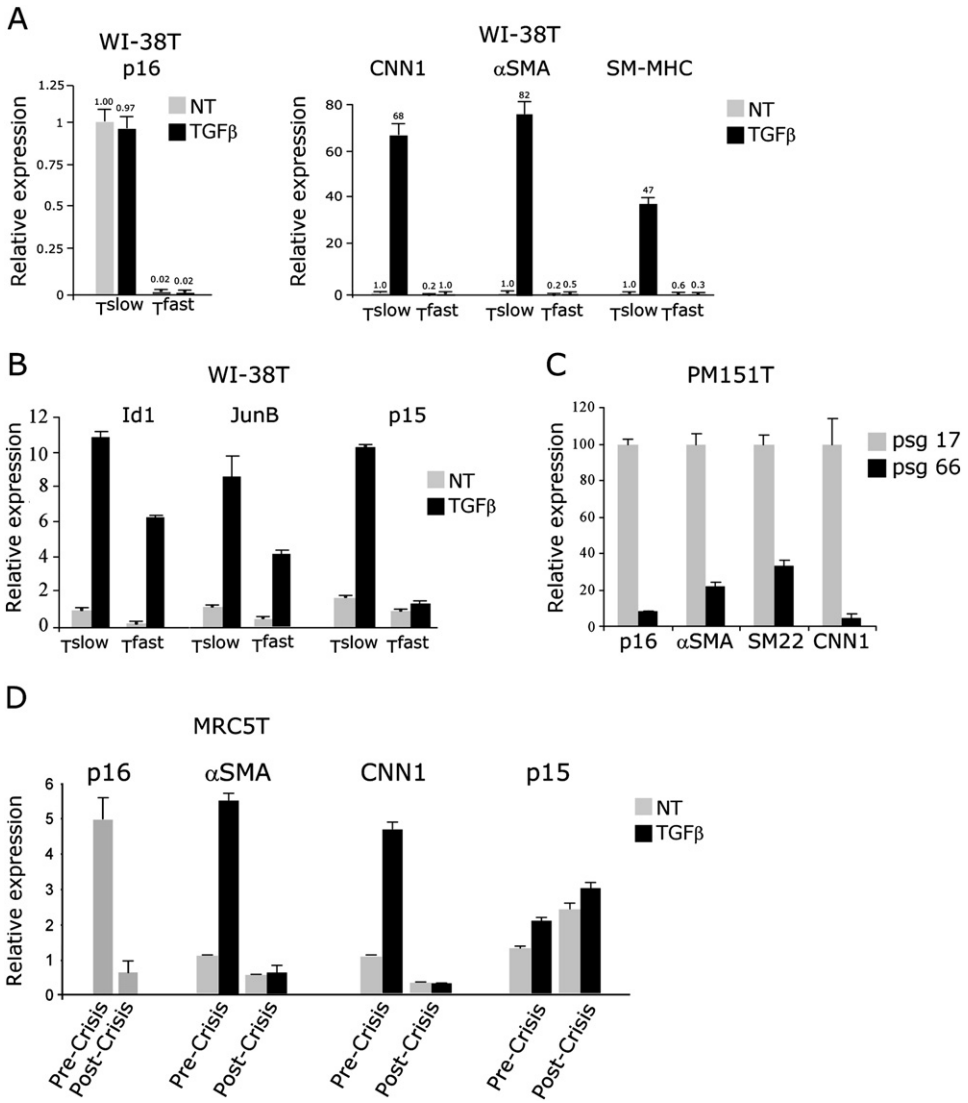

Figure 1. INK4A-Inactivated Human Mesenchymal Cells Have Disrupted Basal and TGFβ-Induced Myofibroblast Differentiation

(A) WI-38 hTERT-immortalized cells from early (T^{slow}) or late (T^{fast}) passages were grown to confluence, serum starved for 24 hr, and then treated with a fresh serum-free medium with 1 ng/ml TGFβ (TGFβ) or without it (NT). Total RNA was isolated 48 hr later for p16, CNN1, and αSMA, and 24 hr later for SM-MHC. Relative expression levels of the indicated genes were determined by QRT-PCR. Values were normalized to the levels of the GAPDH housekeeping control in the same cDNA samples.

(B) Relative expression levels of the indicated genes in the experiment described in (A) were determined by QRT-PCR. Samples for determination of Id1 and JunB levels were collected 2 hr after TGFβ addition, and p15 levels were determined 24 hr after TGFβ addition.

(C) Basal expression levels of p16 and indicated differentiation markers in sparse prostate smooth muscle hTERT-immortalized PM151T cells from early (psg 17) or late (psg 66) passages were determined by QRT-PCR.

(D) TGFβ experiment as in (A) was performed with MRC5 hTERT-immortalized cells (MRC5T) from early (Pre-Crisis) or late (Post-Crisis) passage cultures. Relative expression levels of the indicated genes were determined by QRT-PCR.

The results are presented as a mean ± SD of two duplicate runs from a representative experiment.

TGFβ signaling in a similar manner to WI-38 T^{slow} cells as judged by SMAD2 and ERK1/2 phosphorylation. In addition, induction of an important transcriptional regulator of cytoskeletal genes, SRF, was intact in WI-38 T^{fast} cells (Figure S1 in the Supplemental Data available with this article online).

In conclusion, data obtained from three independent cellular systems demonstrate that p16 inactivation in human mesenchymal cells is associated with the reduced expression of myofibroblast and smooth muscle markers. Furthermore, the myofibroblast differentiation program induced by TGFβ is impaired in p16-negative human fibroblasts. Most probably, this differentiation defect lies downstream of SMAD and ERK1/2 phosphorylation, and it can be dissociated from immediate-early gene induction.

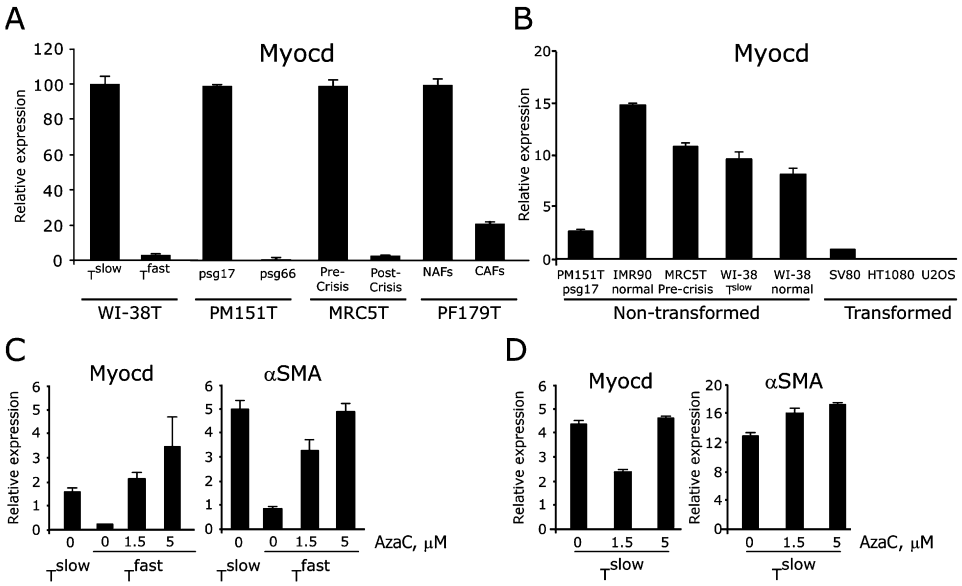

Figure 2. Transformation-Associated Myocardin Gene Repression

(A) Basal expression levels of myocardin in hTERT-immortalized cells from early (WI-38 T^{slow}, PM151T psg17, precrisis MRC5T, and prostate NAFs) or late (WI-38 T^{fast}, PM151T psg66, postcrisis MRC5T, and prostate CAFs) passages were determined by QRT-PCR. The relative expression levels in the early passages were set to 100% for each cell strain.

(B) Basal myocardin mRNA levels were measured in the indicated nontransformed strains and transformed mesenchymal cell lines.

(C) WI-38 T^{fast} or T^{slow} cells were treated with the indicated doses of 5-Azacytidine (AzaC) for 3 days and then released into drug-free medium for an additional 2 days. Relative expression levels of myocardin and αSMA are shown.

(D) Experiment similar to (C) was performed in T^{slow} cells.

The results are presented as a mean ± SD of two duplicate runs from a representative experiment.

Transformation-Associated Myocardin Gene Repression

As our results suggested that the defect in TGFβ-mediated induction of numerous myofibroblast markers in T^{fast} cells lies downstream of SMAD and ERK activation and SRF induction, we reasoned that it could be at the level of SRF transcription cofactor(s). Since myocardin is one such cofactor, known to be important for regulation of multiple smooth muscle and myofibroblast marker genes, we examined its expression levels in our cells. Strikingly, expression of myocardin was dramatically downregulated during prolonged culture in all three cellular systems studied, namely in WI-38T (T^{slow} versus T^{fast}), PM151T (psg 17 versus psg 66), and MRC5T (precrisis versus postcrisis). We also detected reduced myocardin expression in carcinoma-associated fibroblasts (CAFs) isolated from prostate cancer compared to the more distal normal-associated isogenic fibroblasts (NAFs) (Figure 2A). These observations prompted us to measure myocardin expression levels in several cell lines of mesenchymal origin.

We found that myocardin is expressed at very low or undetectable levels in the transformed cell lines U2OS, HT1080, and SV80, compared with the high levels detected in three nontransformed fibroblast strains (IMR90, MRC5, and WI-38) and a prostate smooth muscle-derived (PM151T) strain (Figure 2B).

Thus, in addition to in vitro immortalized and transformed cells, low myocardin expression was also characteristic of primary tumor-derived cell lines.

Promoter methylation is frequently associated with gene silencing in carcinogenesis. To test whether DNA methylation was responsible for myocardin silencing in T^{fast} cells, we treated them with increasing concentrations of the DNA methyltransferase inhibitor AzaC and measured myocardin expression by QRT-PCR. Figure 2C demonstrates that this treatment resulted in a dose-dependent upregulation of myocardin expression in T^{fast} cells. Importantly, reactivation of myocardin was accompanied by a dose-dependent upregulation of αSMA, indicative of myofibroblast differentiation (Figure 2C). Similar treatment of T^{slow} cells did not affect myocardin and αSMA expression significantly (Figure 2D). These results suggest that myocardin promoter repression is a readily reversible dynamic process in premalignant T^{fast} cells.

To directly test the methylation status of myocardin promoter in T^{slow} and T^{fast} cells, we performed a methylation-sensitive PCR assay. Unexpectedly, we found no evidence of myocardin promoter methylation in both T^{slow} and T^{fast} cells. Bisulfite sequencing confirmed lack of DNA methylation at 15 potential CpG methylation sites in the myocardin promoter (Figures S2A and S2B).

In summary, our results show that myocardin is downregulated in premalignant p16-negative immortalized cell strains and in tumor-derived cell lines. Myocardin expression in WI-38 T^{fast} cells could be restored by AzaC treatment; however, DNA methylation does not seem to be involved in myocardin repression.

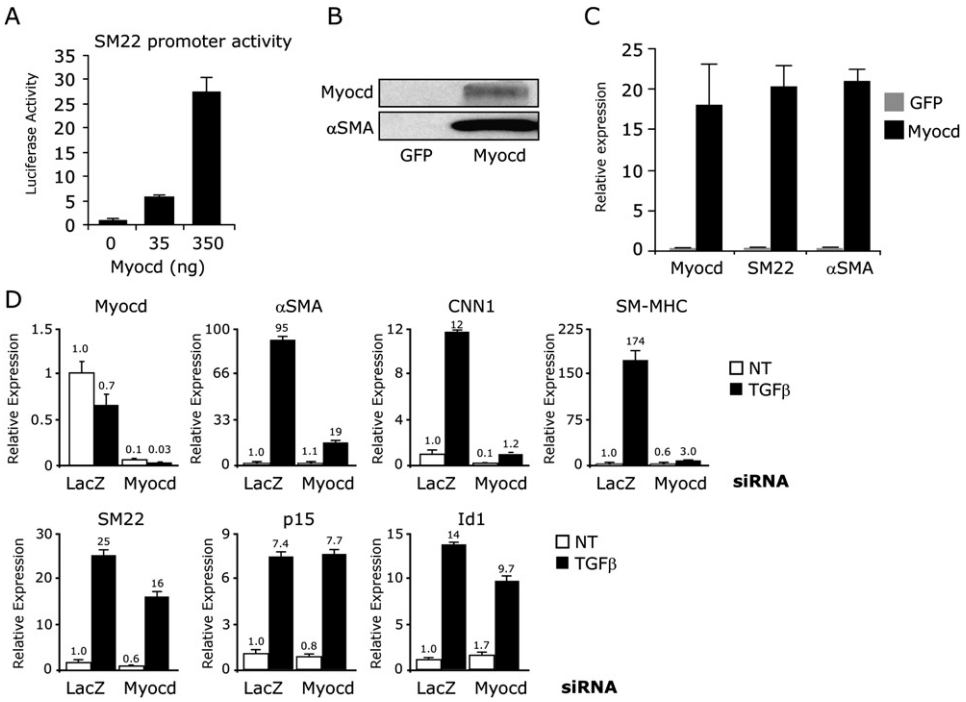

Figure 3. Myocardin Is Necessary and Sufficient for Myofibroblast Differentiation of Human Fibroblasts

(A) WI-38 T^{fast} cells were transiently transfected with 400 ng of SM22-luciferase reporter along with the indicated amounts of myocardin expression plasmid. Luciferase activity was determined 48 hr later and normalized to cotransfected β-gal activity. The results are presented as a mean ± SD of triplicate transfections from a representative experiment. (B and C) Western blot analysis of myc-tagged myocardin and αSMA (B) and QRT-PCR of myocardin, SM22, and α-SMA (C) in HT1080 cells infected with retroviruses encoding myc-tagged myocardin (Myocd) or GFP control (GFP). (D) WI-38 T^{slow} cells were transfected with siRNA duplexes targeting either myocardin (Myocd) or LacZ (LacZ). Twenty-four hours later, cells were serum starved for 24 hr and then treated with TGFβ or control serum-free medium (NT) for an additional 24 hr. Relative expression levels of the indicated genes were determined by QRT-PCR. The results of QRT-PCR are presented as a mean ± SD of two duplicate runs from a representative experiment.

Myocardin Is Necessary and Sufficient for Myofibroblast Differentiation of Human Fibroblasts

To examine the functional role of myocardin in differentiation and transformation, we first tested the ability of ectopically expressed myocardin to induce the activity of a prototype SM and myofibroblast promoter, SM22, in WI-38 T^{fast} cells (Du et al., 2003). Indeed, we found that myocardin transactivates this reporter in a dose-dependent manner (Figure 3A).

To assess the effect of ectopic expression of myocardin on the endogenous levels of differentiation markers, we infected human fibrosarcoma cell line HT1080 with retroviruses expressing either the full-length myocardin or the GFP control protein. Following selection, expression of the transgene was verified by Western blotting (Figure 3B). While HT1080 cells infected with the GFP control expressed undetectable levels of myocardin mRNA and other smooth muscle markers, ectopic expression of myocardin resulted in a dramatic induction of SM22 and αSMA differentiation markers (Figures 3B and 3C). Collectively, these results indicate that expression of myocardin is sufficient for the induction of a smooth muscle gene expression program in human mesenchymal cells.

Next, we examined the requirement of the endogenous myocardin for basal and TGFβ-induced expression of myofibroblast markers in WI-38 fibroblasts. Knockdown of myocardin using specific siRNA resulted in a reduction in basal levels, and attenuation of TGFβ-mediated induction of the differentiation markers αSMA, CNN1, SM-MHC, and SM22. Importantly, this effect was specific for differentiation-associated genes, as induction of other TGFβ targets, such as p15 and Id1, was not affected (Figure 3D). These results demonstrate that myocardin is necessary for basal and TGFβ-induced expression of myofibroblast markers in WI-38 cells and provide strong evidence that loss of myocardin during transformation of these cells represents the basis for the observed differentiation block.

Myocardin Is Induced by Serum Withdrawal and TGFβ

Having demonstrated the pivotal role of myocardin in basal and TGFβ-mediated differentiation of WI-38 cells, we then investigated the regulation of myocardin itself in more detail. To this end, we measured changes in myocardin expression following TGFβ treatment of proliferating versus serum-deprived WI-38 T^{slow} cells (Figure 4A). In parallel, cell proliferation status was monitored using a bromodeoxyuridine (BrdU) incorporation assay. We found that serum deprivation accompanied by the establishment of the quiescence state resulted in a significant induction of

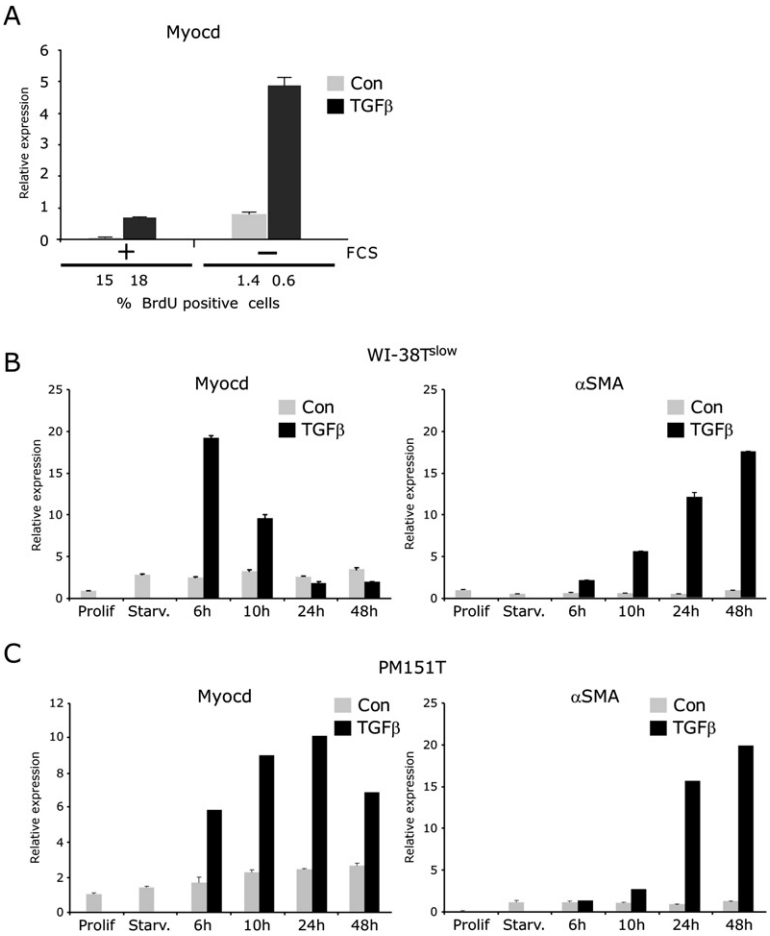

Figure 4. Myocardin Is Induced by Serum Withdrawal and TGFβ

(A) WI-38 T^{slow} cells were serum starved for 24 hr (–) or grown in a full serum-containing medium (+). Then TGFβ or the corresponding control medium was added for 6 hr. Myocardin mRNA levels were determined by QRT-PCR, and the proportion of cells in S phase of the cell cycle was determined by the BrdU incorporation assay.

(B and C) WI-38 T^{slow} cells (B) and PM151T psg 22 cells (C) were serum starved for 24 hr and then treated with TGFβ or mock treated for the indicated times. Relative expression levels of myocardin and αSMA were determined by QRT-PCR.

The results of QRT-PCR are presented as a mean ± SD of two duplicate runs from a representative experiment.

myocardin mRNA. Subsequent treatment of quiescent cells with TGFβ induced an additional robust increase in myocardin expression. Notably, myocardin was induced to significantly lower levels when TGFβ treatment was applied to the cells proliferating in the presence of serum.

Next, we investigated the kinetics of myocardin induction during the course of the TGFβ treatment. As shown in Figure 4B, myocardin was significantly upregulated following serum starvation of WI-38 T^{slow} cells, and TGFβ treatment resulted in an additional robust induction of myocardin peaking at 6 hr, followed by a gradual decline to the basal levels by 24 hr. This transient pattern of myocardin induction explains the fact that we did not detect elevation of myocardin mRNA levels in the experiment shown in Figure 3D, where the samples were collected at 24 hr time points. Similarly, myocardin was gradually induced by serum starvation and TGFβ treatment in the early passage of prostate SMCs (PM151T psg 24), further substantiating our findings (Figure 4C). Notably, in both cell types myocardin mRNA induction preceded that of αSMA, suggesting that transcriptional induction of myocardin is an important step in the induction of myofibroblast differentiation induced by TGFβ. In summary, we have shown that myocardin mRNA levels are positively regulated by serum withdrawal and TGFβ.

A Contact Inhibition Defect of T^{fast} Cells Counteracts TGFβ-Mediated Differentiation

We have previously described that WI-38 T^{fast} cells are characterized by a contact inhibition defect that enables them to reach a saturation density up to 7-fold higher than that of T^{slow} cells (Milyavsky et al., 2003). To test the effect of cell density on the TGFβ-mediated differentiation, we performed an experiment in sparse and dense cultures of WI-38 T^{slow} and T^{fast} cells. We found that serum deprivation of sparse cultures resulted in an almost complete inhibition of DNA synthesis in both T^{slow} and T^{fast} cells (Figure 5A).

However, a different situation was observed in the confluent conditions. While T^{slow} cultures completely ceased proliferation, dense WI-38 T^{fast} cells lost their capacity to exit the cell cycle upon serum withdrawal and TGFβ treatment (Figure 5A).

Addition of TGFβ resulted in myocardin induction and robust αSMA upregulation in dense cultures of T^{slow} cells, but not of T^{fast} cells (Figure 5B). Strikingly, we found that under sparse conditions TGFβ upregulated myocardin and αSMA in T^{fast} cells. However, the induced level of αSMA was much lower in T^{fast} compared with T^{slow} cells as measured by both QRT-PCR and Western blotting consistently with the partial upregulation of

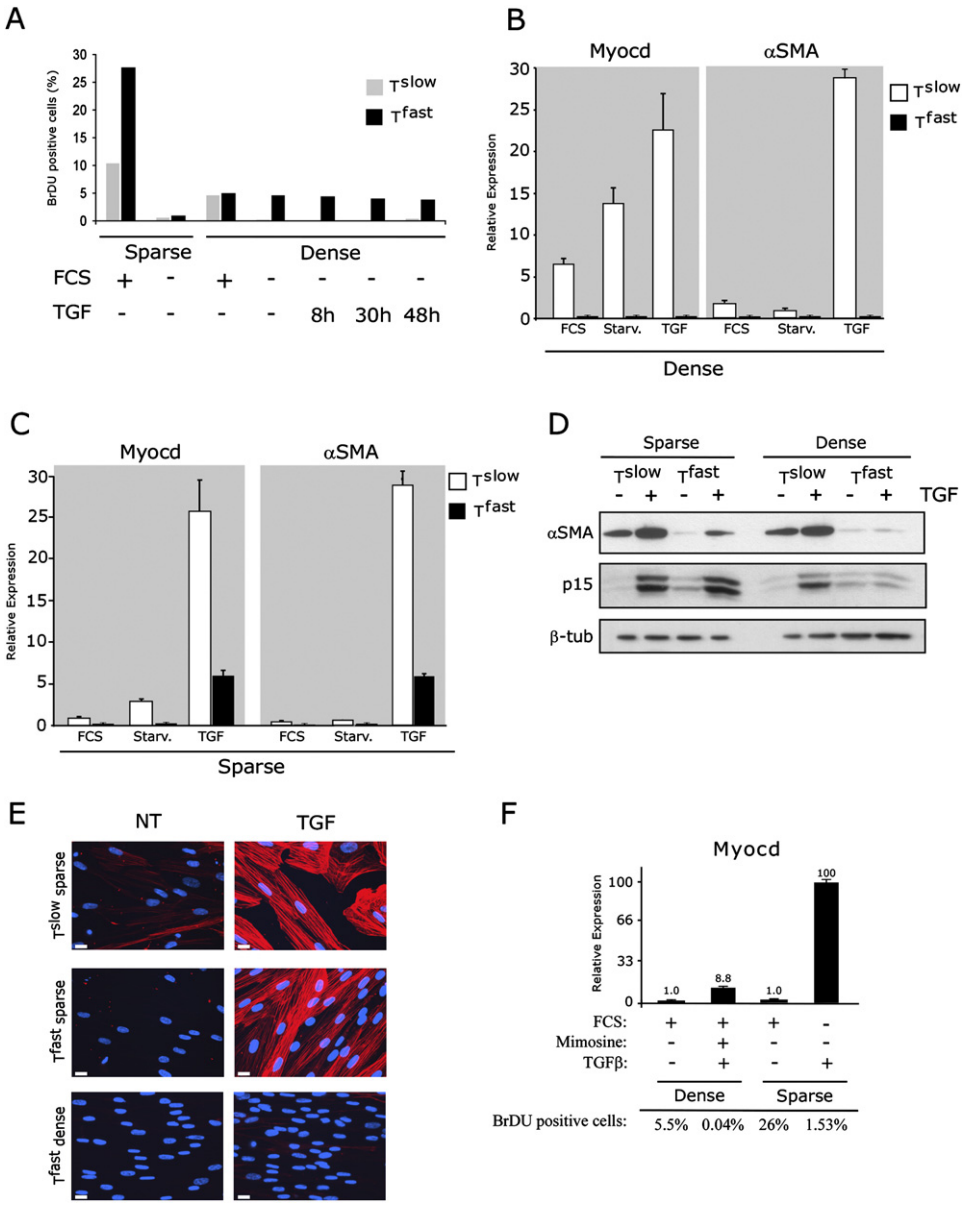

Figure 5. A Contact Inhibition Defect Counteracts TGFβ-Mediated Differentiation

(A) WI-38 hTERT-immortalized cells from early (T^{slow}) or late (T^{fast}) passages were grown in sparse or dense conditions, with (+) or without (–) FCS. Where indicated, serum-starved dense cultures were treated for the indicated times with a fresh starvation medium containing TGFβ. The proportion of cells in S phase of the cell cycle was determined by BrdU incorporation assay.

(B) WI-38 T^{slow} and T^{fast} cells were grown to high density in a full serum-containing medium (FCS), then serum starved for 24 hr (starv.) and treated with TGFβ for 4 hr (for myocardin) or 24 hr (for αSMA) determination. Relative expression levels of myocardin and αSMA were measured by QRT-PCR.

(C) Same experiment as in (B) was performed in sparse cells.

(D) Western blot of αSMA, p15, and β-tubulin (loading control) in sparse and dense WI-38 cells that were serum starved for 24 hr and treated either with TGFβ (+) or control medium (–) for 30 hr.

(E) Immunofluorescent staining for αSMA (red) and DAPI (blue) in sparse and dense WI-38 T^{fast} cells and dense T^{slow} cells that were serum starved for 24 hr and treated either with TGFβ or control medium (NT) for 24 hr. Scale bars, 15 μm.

(F) WI-38 T^{fast} confluent or sparse cells were arrested by 0.5 mM mimosine (confluent cells) or by serum deprivation (sparse cells) for 24 hr and then treated with TGFβ or control medium for 24 hr. Relative expression levels of myocardin and proportion of cells in S phase are indicated.

The results of QRT-PCR are presented as a mean ± SD of two duplicate runs from a representative experiment.

myocardin mRNA (Figures 5C and 5D). Immunofluorescence of αSMA protein in sparse T^{fast} cells treated with TGFβ revealed changes in cell shape and the development of actin cables, indicative of functional differentiation. In agreement with our previous findings, TGFβ treatment of dense cultures of T^{fast} cells failed to

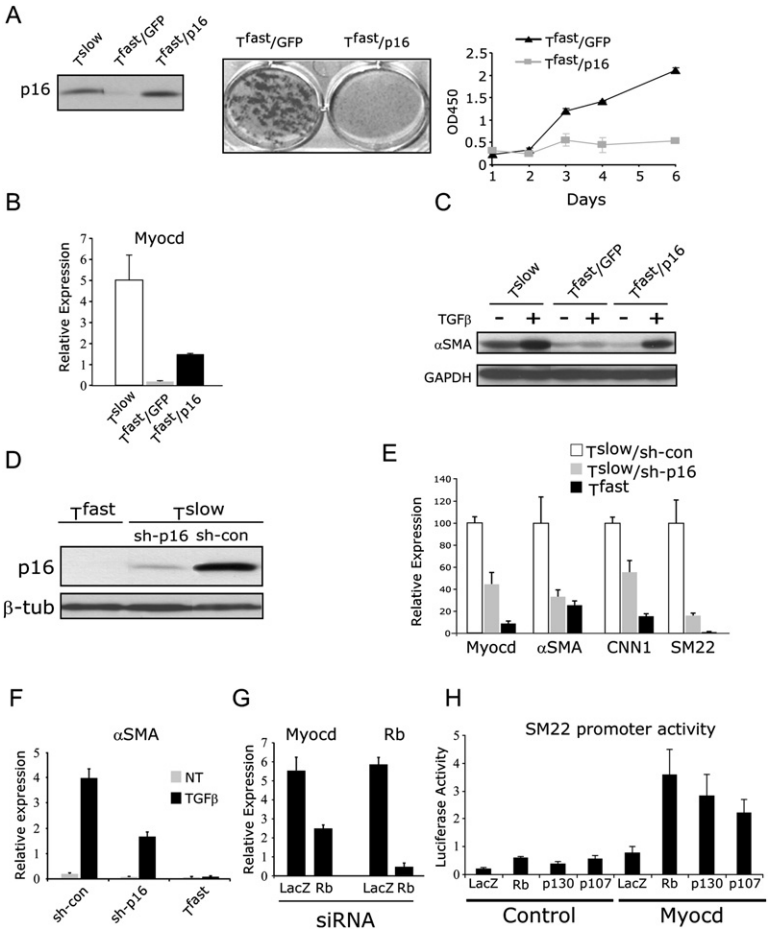

Figure 6. p16 and Pocket Proteins Are Involved in the Regulation of Myocardin and Myofibroblast Differentiation

(A) Western blot analysis of p16 (left panel), proliferation (right panel), and colony forming assays (middle panel) of WI-38 T^{fast} cells infected with retroviruses encoding p16 (T^{fast}/p16) or GFP (T^{fast}/GFP). The results of the WST1 cell proliferation assay are presented as a mean ± SD of triplicate wells from a representative experiment. (B) Basal expression levels of myocardin in sparse cells described in (A) grown in a full serum-containing medium. (C) Western blot of αSMA and GAPDH (loading control) in cells described in (A) following 24 hr treatment of dense cells with TGFβ (+) or control medium (−). (D) Western blot analysis of p16 in WI-38 T^{fast} cells and T^{slow} cells infected with retroviruses encoding shRNA targeting p16 (sh-p16) or control shRNA (sh-con). β-tubulin serves as a loading control. (E) Basal expression levels of myocardin and the indicated differentiation markers in sparse cells described in (D) grown in a full serum-containing medium. (F) QRT-PCR of αSMA in cells described in (D) following 48 hr treatment of dense serum-starved cells with TGFβ or control medium (NT). (G) WI-38 T^{slow} cells were transfected with siRNA oligonucleotide duplexes targeting Rb or LacZ. Relative expression levels of Rb and myocardin were determined by QRT-PCR. For (B) and (E)–(G), the results are presented as a mean ± SD of two duplicate runs from a representative experiment. (H) Saos-2 cells were transiently cotransfected with 300 ng of SM22 promoter reporter and 100 ng of the indicated expression plasmids for pocket proteins or LacZ control either with or without 5 ng of myocardin expression plasmid. Twenty-four hours later, cells were serum starved for an additional 24 hr, and reporter activity was determined. Transfection efficiency was normalized on the basis of the activity of the cotransfected renilla luciferase. The results are presented as a mean ± SD of triplicate transfections from a representative experiment.

induce cytoskeleton rearrangement and αSMA staining (Figure 5E).

In contrast to only partial restoration of myofibroblast markers and TGFβ-mediated induction of myocardin in sparse T^{fast} cells, induction of p15 was completely restored in sparse cultures of T^{fast} cells, suggesting that p15 and cytoskeletal markers are differentially regulated by TGFβ (Figure 5D). In order to characterize the role of growth arrest in TGFβ-induced differentiation, we used a plant amino acid, mimosine, that induces cell-cycle arrest in late G1. Mimosine-arrested dense T^{fast} cells failed to induce myocardin (Figure 5F) and αSMA (data not shown) upon TGFβ treatment, unlike sparse T^{fast} cells arrested by serum starvation. Thus, the inability to attain complete growth arrest following serum deprivation is not likely to be responsible for the differentiation block observed in dense T^{fast} cells.

Taken together, our results demonstrate that a contact inhibition defect of T^{fast} cells abrogates the induction of myocardin by TGFβ and the subsequent differentiation.

p16 and Pocket Proteins Are Involved in the Regulation of Myocardin and Myofibroblast Differentiation

Our data obtained from three independently immortalized cell lines demonstrate a correlation between p16 silencing and downregulation of SM differentiation markers and myocardin (Figures 1A, 1C, and 1D). To elucidate the specific role of p16 in myofibroblast differentiation, we studied the effects of ectopic p16 restoration in WI-38 T^{fast} cells. Retrovirally transduced p16 was detected at a slightly higher level than endogenous p16 in early-passage T^{slow} cells (Figure 6A, left panel). This resulted in inhibition of cell proliferation in a short-term growth assay (Figure 6A, right panel) and complete elimination of the colony forming capacity of T^{fast} cells (Figure 6A, middle panel). Most importantly, p16 re-expression in T^{fast} cells resulted in upregulation of basal levels of myocardin (Figure 6B). Interestingly, p15 ectopic expression in T^{fast} cells similarly resulted in elevation of myocardin mRNA (Figure S5). Furthermore, TGFβ-induced αSMA upregulation was restored by ectopic expression of p16 in dense T^{fast} cells (Figure 6C).

As a complementary approach to evaluate the role of p16 in the process of myofibroblast differentiation, we knocked down the expression of endogenous p16 using shRNA. Transduction of T^{slow} cells with the retrovirus encoding p16-directed shRNA (T^{slow}/sh-p16) resulted in approximately 90% reduction in the p16 protein level (Figure 6D) and in decreased basal myocardin expression (Figure 6E). This was accompanied by a reduction of basal levels of αSMA, CNN1, and SM22 mRNAs (Figure 6E). Next, we examined the effect of p16 knockdown on TGFβ-induced differentiation. Figure 6F demonstrates that treatment of confluent and serum-deprived cultures of T^{slow}/sh-p16 cells resulted in impaired induction of differentiation, as evidenced by the attenuated αSMA upregulation compared with the T^{slow}/sh-con cells. Collectively, these results demonstrate that p16 is an upstream regulator of myocardin expression and that p16 loss may contribute to differentiation defects through myocardin downregulation.

Since both p16 and serum deprivation ultimately lead to growth arrest through activation of Rb tumor suppressor, we examined the possible involvement of Rb in myocardin regulation by knocking down Rb expression in WI-38 T^{slow} cells. As shown in Figure 6G, transfection of these cells with siRNA duplexes directed against Rb resulted in a significant downregulation of myocardin mRNA levels.

To determine whether the AzaC effect on myocardin reactivation in T^{fast} cells (Figure 2C) is downstream of p16 re-expression and subsequent activation of the pRb pathway, we knocked down the expression of Rb or p16 in T^{fast} cells. Then we treated these cells together with their counterparts infected with the control shRNA with AzaC and monitored myocardin expression. Our results demonstrate that knockdown of either Rb or p16 abrogated myocardin induction following AzaC treatment (Figure S3).

Next, we tested whether downstream targets of p16, namely pRb, p107, or p130 may cooperate with myocardin during the induction of the differentiation transcriptional program. To test this possibility, we cotransfected SM22 promoter reporter construct together with the above-mentioned pocket proteins into Rb-negative Saos-2 cells. All three pocket proteins were found to upregulate the activity of this prototype SM promoter, confirming their role in the regulation of smooth muscle genes (Figure 6H). Most importantly, all three pocket proteins cooperated with the exogenous myocardin in activation of this promoter. These results suggest that, in addition to the regulation of myocardin mRNA, pocket proteins also cooperate with myocardin protein during transcriptional activation of SM promoters.

Collectively, these results indicate that p16 and pocket proteins positively regulate myocardin expression and activity, which potentially explains the contribution of p16 loss to differentiation defects.

Antiproliferative Activity of Myocardin

Differentiation defects are one of the most common features of cancer cells. Thus, our findings regarding the key role of myocardin in myofibroblast differentiation and its frequent downregulation during immortalization and transformation processes prompted us to assess the effect of ectopic expression of myocardin on growth characteristics of HT1080 fibrosarcoma cells (Figures 3B and 3C). Interestingly, we found that the growth rate of myocardin-expressing cells was similar to that of GFP-expressing control cells when measured under standard culture conditions at relatively high cell density (data not shown). However, when the cells were seeded at a lower density of 1000 cell/cm^2, myocardin-expressing cells underwent a complete growth inhibition (Figure 7A). Similarly, myocardin expression completely abrogated the colony forming ability of HT1080 cells (Figure 7B). Anchorage-independent growth is an established assay to assess the malignant potential of cells. As demonstrated in Figure 7C, ectopic expression of myocardin entirely abolished the ability of HT1080 cells to form colonies in soft agar.

In agreement with the results obtained in HT1080 cells, myocardin restoration in a tumor cell line created from oncogenically transformed WI-38 T^{fast} cells was able to block tumor cell growth in vitro and restore expression of SM22 and CNN1 (Figure S4).

To determine the effects of endogenous myocardin on growth characteristics of WI-38 T^{slow} cells, we inactivated it by two independent techniques. Figure 7D demonstrates that cells infected with a dominant-negative myocardin form acquired enhanced proliferative potential as manifested by a colony forming assay. Similar results were obtained when myocardin was knocked down using RNA interference (Figure 7E). Notably, the colony forming ability was significantly higher in prostate-derived CAFs with reduced myocardin levels (Figure 2A) compared with the more distal fibroblasts from the same patient (Figure 7F). In summary, these results demonstrate antiproliferative activity of myocardin in human mesenchymal cells.

Characterization of Myocardin Expression in Human Tumors

To further examine the hypothesis that myocardin repression is a frequent event during malignant transformation, we searched the Oncomine database (Rhodes et al., 2004) for clinical tumor samples that have significant downregulation of myocardin expression compared with the corresponding normal tissues. As demonstrated in Figure 8A, we found that myocardin was significantly downregulated in prostate and colon tumor samples compared with normal tissue controls (Dhanasekaran et al., 2001; Lapointe et al., 2004; Zou et al., 2002).

Next, we examined myocardin expression in matched pairs of cDNA prepared from tumor and adjacent normal tissue derived from individual patients by dot blot analysis using the Cancer Profiling Array. One hundred and fifty-four matched pairs representing different cancer tissues were hybridized with myocardin-specific probe (Figure 8B). Specificity of myocardin probe was validated by northern blot analysis in T^{slow} and T^{fast} cells. As expected,

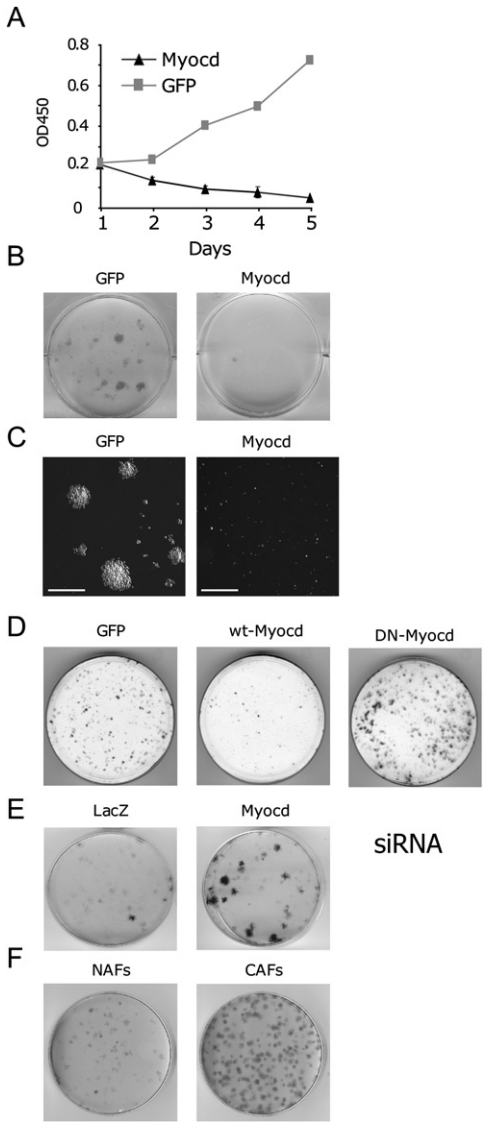

Figure 7. Antiproliferative Activity of Myocardin

(A–C) WST1 proliferation (A), colony forming (B), and soft agar (C) assays of HT1080 cells infected with retroviruses encoding myc-tagged myocardin (Myocd) or GFP control described in Figure 3B. Scale bar, 1 mm. The results of the WST1 cell proliferation assay are presented as a mean ± SD of triplicate wells from a representative experiment.

(D) WI-38/T^{slow} cells were infected with retroviruses encoding either wild-type (wt-Myocd) or dominant-negative (DN-MyocD) myocardin forms or GFP and plated for colony forming assay.

(E) WI-38/T^{slow} cells were transfected with siRNA duplexes targeting either myocardin (Myocd) or LacZ (LacZ) control and 2 days later plated for colony forming assay.

(F) Comparable passages of prostate fibroblasts isolated from non-malignant (NAFs) or carcinoma-adjacent areas (CAFs) were plated for colony forming assay.

T^{fast} cells exhibited diminished expression of myocardin as compared with T^{slow} cells (Figure S6). Array analysis revealed clear reduction in myocardin expression in colon (9/10), cervix (9/10), uterus (8/10), and rectum (5/10) cancer samples (Figure 8B).

Although myocardin reduction in colon cancer was detected by both methods, its reduced expression in prostate tissue was evident only from a bioinformatics survey. Importantly, Oncomine results were extracted from two independent studies that compared 62 prostate cancer samples with 41 normal prostate controls (Lapointe et al., 2004) and 59 prostate cancer samples with 16 benign prostate hyperplasias (BPH) and 6 normal prostate tissues (Dhanasekaran et al., 2001). Therefore, one plausible explanation for this apparent discrepancy might stem from the small number of prostate cancer cDNAs presented on the Cancer Profiling Array. It is equally possible that differences existed between the methodologies used for tissue harvesting, processing, and normalization in the studies referenced in Oncomine and in the Cancer Profiling Array.

To determine whether the reduced myocardin levels are attributable to the overrepresentation of epithelial compartment in tumor samples or reflect changes in the malignant stroma, we reprobed the membrane with a pan-mesenchymal marker, vimentin. As is evident from Figure 8B, vimentin expression was not significantly changed in those tumor samples, in which significant myocardin reduction was detected. Thus, we conclude that reduced myocardin expression in some epithelial tumors reflects changes in the tumor stroma.

Finally, we characterized myocardin expression at the cellular level in vivo using mRNA in situ hybridization in a panel of soft tissue tumors and adjacent normal tissues. Myocardin-specific signal was abundantly detected in normal fibrous and aorta-derived tissues, most probably corresponding to the myofibroblasts and SMCs (Figure 8C). On the other hand, myocardin expression was undetectable or low in 43% (3/7) leiomyosarcomas, 33% (1/3) malignant blood vessel tumors, and 22% (3/14) of fibrous tissue tumors. Representative samples of negative leiomyosarcomas (A8 and B5) are shown. Notably, in some leiomyosarcomas (sample B1) and in giant cell type malignant fibrous histiocytoma (sample G6), we detected intratumor heterogeneity in myocardin expression. In those cases, regions composed of poorly differentiated malignant cells contained less myocardin signal than more highly differentiated malignant counterparts (Figure 8C).

Based on the combined evidence from all three independent in vivo approaches, together with the ability of myocardin to inhibit the malignant phenotype of fibrosarcoma cell lines and to restrict proliferation of primary fibroblasts, we conclude that myocardin is an important constituent of the growth-regulatory circuit aimed to protect cells from malignant transformation.

DISCUSSION

Although the key role of myocardin in the processes of cardiac and smooth muscle development is firmly established, its involvement in the neoplastic process was not previously addressed. Our study provides experimental evidence to support the involvement of myocardin in carcinogenesis. Our results indicate that the long-known

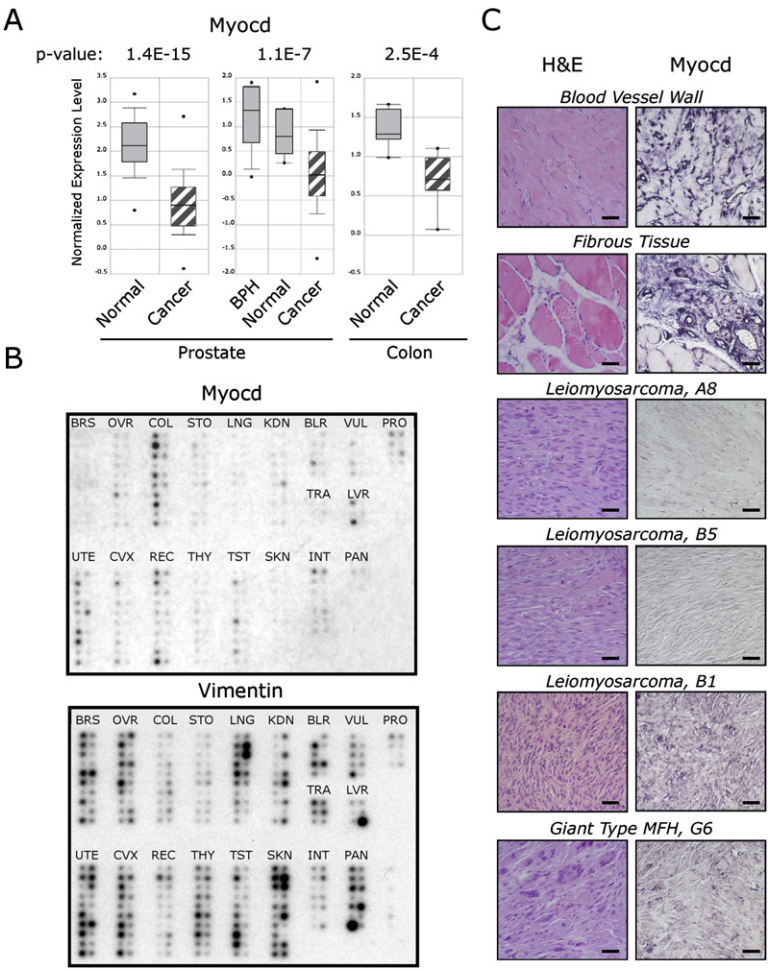

Figure 8. Analysis of Myocardin Expression In Vivo

(A) The Oncomine database was queried for studies, in which myocardin expression significantly differs between cancer and normal samples. The p value designates the probability that the observed difference in myocardin expression between normal and cancer samples is due to random chance. The studies with the lowest p values are shown. The bars represent 25%–75% interval of normalized myocardin expression levels in each group. The deviation lines represent 10%–90% interval, and dots represent samples with minimum and maximum expression level in a given group.

(B) Dot blot analysis of myocardin and vimentin expression in cancer versus normal tissues using cancer profiling array. Left and right columns for every tumor type correspond to the cDNA from nonmalignant and tumor tissues, respectively. BRS, breast; OVR, ovary; COL, colon; STO, stomach; LNG, lung; KDN, kidney; BLR, bladder; VUL, vulva; PRO, prostate; TRA, trachea; LVR, liver; UTE, uterus; CVX, cervix; REC, rectum; THY, thyroid gland; TST, testis; SKN, skin; INT, small intestine; PAN, pancreas. Detailed sample description accompanied by H&E stainings of the samples used for cDNA preparation can be found at http://bioinfo2.clontech.com/dparray/array-list-action.do and then choosing Cancer Profiling Array II.

(C) Myocardin mRNA expression by in situ hybridization analysis using tissue array of human soft tissue tumors. Violet staining indicates the presence of myocardin mRNA. H&E staining prepared from the same specimen is also shown. Scale bars, 50 μm. High-resolution images are included in Figure S7.

observation of the reduced expression of smooth muscle differentiation markers during transformation may be due to the inactivation of their master transcriptional regulator, myocardin. Our data indicate that myocardin expression and function in primary cells are tightly regulated by cell-growth mechanisms that are involved in mitogen sensing and contact inhibition.

The importance of cell density and quiescence for growth arrest and differentiation has been noted in several studies (Halevy et al., 1995; Thomas et al., 2001). It is thought that the cell-cell contact that occurs in high-cell-density cultures closely recapitulates tissue architecture. Although many signaling components of contact-mediated growth arrest are still unknown, there is evidence that p16, pocket proteins, and p53 are involved in the establishment and the maintenance of this process (Meerson et al., 2004; Wieser et al., 1999; Zhang et al., 1999). We and others have shown that premalignant fibroblasts that lost p16 acquired a contact inhibition defect. Our results indicate that the defect in contact inhibition and subsequent loss of sensitivity to mitogen withdrawal impedes the induction of myocardin and TGFβ-mediated differentiation. It is possible that the specific stage of the cell-cycle arrest that is achieved by mitogen withdrawal in the cells with intact p16/Rb, but could not be recapitulated by late G1 arrest inducers, such as mimosine, is important for myocardin induction.

A positive effect of p16 and Rb proteins on the basal myocardin and its target gene expression, together with functional cooperation between myocardin and Rb/p130/p107 pocket proteins in transactivation of a prototype smooth muscle promoter, provides an additional mechanism for p16/Rb-mediated regulation of differentiation in fibroblasts. In agreement with our findings, reduced myocardin levels were found in early embryoid bodies generated from Rb knockout stem cells (Papadimou et al., 2005). We therefore speculate that myocardin regulation by p16 in this differentiation process is at least partially responsible for p16 tumor-suppressor function. Indeed, p16 null mice develop sarcomas, among other malignancies (Krimpenfort et al., 2001; Sharpless et al., 2001).

The mechanism by which TGFβ induces transcription of smooth muscle differentiation markers is not completely understood. Our finding that myocardin is a transcriptional target of TGFβ enables us to propose that transcriptional induction of myocardin is an important previously unrecognized step, required for the induction of myofibroblast/SMCs differentiation targets by TGFβ. We found that

SRF protein levels are downregulated by serum starvation and increase upon TGFβ treatment (Figure S1), correlating with αSMA induction. These observations, combined with the published data in the field and our myocardin siRNA data (Figure 3D), suggest that upregulation of both myocardin and SRF are necessary for αSMA induction.

Robust antiproliferative activity of myocardin in vitro as well as its reduced expression in some primary sarcomas and in the tumor stroma set the ground for further studies on myocardin function in the carcinogenic process. The fact that the close myocardin homolog MKL1 is frequently involved in oncogenic fusions in megakaryoblastic leukemia provides an additional piece of circumstantial evidence for the role of myocardin in cancer (Ma et al., 2001). Our results suggest that myocardin might act as a downstream mediator of tumor-suppressive functions of p16/Rb and/or TGFβ in some tumor types. It is clear, however, that additional transformation-related pathways regulate myocardin levels and activity. The possibility that in a subset of cancers myocardin acts as an independent tumor suppressor targeted by mutations or epigenetically silenced also requires further investigation. Since myocardin knockout is embryonically lethal due to severe defects in vascular development (Li et al., 2003), conditional or tissue-specific knockouts are needed for further studies of the myocardin role in transformation.

The role of myocardin in human carcinogenesis demonstrated in this study has potentially important basic and clinical implications. First, myocardin loss may be a frequent event and a powerful oncogenic trigger not only in mesenchymal, but also in epithelial, tumorigenesis. Second, pharmacological reactivation of myocardin may represent a promising therapeutic strategy, consistent with the proven transformation-suppressive role of its direct target, calponin (Horiuchi et al., 1999). Finally, myocardin targets such as αSMA and calponin are widely used as markers in sarcoma diagnosis and classification, where low calponin expression correlates with aggressive clinical behavior of human angiomyolipoma and osteosarcoma (Islam et al., 2004; Yamamura et al., 1998). Thus, evaluation of myocardin status might represent a valuable diagnostic and prognostic factor in sarcoma.

In summary, our results provide mechanistic insights to myocardin regulation and demonstrate that, in addition to its well-recognized function in development and differentiation, myocardin plays an important role in the process of malignant transformation.

EXPERIMENTAL PROCEDURES

Cell Culture and Treatments

The primary human embryonic lung fibroblasts WI-38 and MRC-5 as well as their hTERT-immortalized derivatives (MacKenzie et al., 2000; Milyavsky et al., 2003, 2005; Taylor et al., 2004), hTERT-expressing normal fibroblasts (NAFs) and carcinoma-associated prostate fibroblasts (CAFs) (strain PF179T), and IMR90 human primary fibroblasts were cultured in MEM supplemented with 10% FCS, 1 mM sodium pyruvate, 2 mM L-glutamine, and antibiotics. HT1080 and SV80 fibrosarcoma and Saos-2 and U2OS osteosarcoma cell lines were maintained in DMEM supplemented with 10% FCS and antibiotics.

hTERT-immortalized (PM151T) human prostate SMCs were grown as described in Kogan et al. (2006).

All cells were maintained in a humidified incubator at 37°C and 5% CO_2.

5-Azacytidine (AzaC) and mimosine were purchased from Sigma.

Retroviral Infections

Retrovirus infection procedures using Phoenix producing cells have been described in detail in Milyavsky et al. (2003).

Plasmids and siRNA

pcDNA3.1-myocardin-myc encoding the full-length myc-tagged version of mouse myocardin, pcDNA3.1-DN-myocardin-myc encoding dominant-negative form of mouse myocardin and SM22-luciferase reporter were provided by Dr. Olson (The University of Texas Southwestern Medical Center, Dallas, TX).

The pRetroSuper-Hygro (pRSH) construct for stable shRNA expression and pRSH-sh-p16^{INK4A} was provided by Dr. Agami (The Netherlands Cancer Institute, Amsterdam, The Netherlands). pRS-sh-con that is directed specifically against murine p63 protein was used as a control shRNA.

pWZL-blasticidin and pWZL-GFP-blasticidin vectors were provided by Dr. Hahn (Dana-Farber Cancer Institute Boston, MA). pcDNA3-pRb, pCMV-p107, and pCMV-p130 were provided by Dr. Ginsberg (Bar-Ilan University, Israel), pCMV5-p15 was provided by J. Massague (Memorial Sloan-Kettering Cancer Center, New York, NY).

pWZL-p16^{INK4A}-blasticidin, pWZL-MyocD-myc-blasticidin, pWZL-DN-MyocD-myc-blasticidin, and pBabe-p15-Hygro constructs are described in the Supplemental Data.

The targeted sequences for shRNAs and synthetic RNAi duplexes are provided in the Supplemental Data.

Reporter Gene Assays

For reporter gene assays, cells were transfected with Fugene 6 Transfection Reagent (Boehringer Mannheim). Cell extracts were prepared 48 hr after transfection, and firefly and Renilla luciferase activities were determined using Promega materials and procedures. The results are presented as a mean ± SD of normalized promoter activity of triplicate wells from a representative experiment.

Quantitative Real-Time PCR

Total RNA was isolated using the RNAeasy kit (Qiagen) according to the manufacturer's protocol. A 2 μg aliquot of the total RNA was reverse transcribed using MMLV RT (Promega) and random hexamer primers. QRT-PCR was performed using SYBR Green PCR Master Mix (Applied Biosystems) on ABI 7000 instrument (Applied Biosystems). The values for the specific genes were normalized to the GAPDH housekeeping control. Primer sequences used in this study are provided in the Supplemental Data. The results are presented as a mean ± SD of two duplicate runs from a representative experiment.

TGFβ-Mediated Induction of Myofibroblast Differentiation

For experiments in dense conditions, cells were grown to visual confluence in 6 cm plates. For experiments in sparse conditions, 10^5 cells were seeded in 6 cm plates 2 days before starvation initiation. When starvation is indicated, cells were washed twice with PBS and changed to serum-free medium for 24 hr. Cells were exposed to 1 ng/ml TGFβ-1 (R&D Systems, Abingdon, UK) for the time periods indicated in the figure legends.

Western Blotting Analysis

The following primary antibodies were used: smooth muscle α-actin (Clone 1A4, Sigma); β-tubulin (Sigma); GAPDH (Chemicon MAB374); p16, p15, and SRF (Santa Cruz Biotechnology); and phospho-Smad2 (Ser465/467) and anti-total SMAD2/3 (Cell Signaling Technology). α-myc antibody was a gift from Dr. Peles (Weizmann Institute of Science, Israel). Anti-phospho-ERK1/2 antibody was a gift from

Dr. Seger (Weizmann Institute of Science, Israel). Detailed description of antibodies is provided in the Supplemental Data.

BrdU Incorporation Assay

Cells were labeled for 30 min with 10 μm of BrdU (Sigma) and stained with FITC-conjugated anti-BrdU (Becton Dickinson) as described elsewhere (Milyavsky et al., 2003) and detailed in the Supplemental Data.

Immunofluorescence

Immunofluorescence of αSMA was performed essentially as described by Chambers et al. (2003).

Cell Proliferation Assay

The commercial WST1 cell proliferation assay was done according to the manufacturer's procedure (Roche Diagnostics, Mannheim, Germany). The values represent mean ± SD of triplicate wells from a representative experiment.

Colony Forming Assay

Four thousand HT1080 cells per well of a six-well plate or 2000 WI-38 or 500 PF179T cells per 6 cm plate were seeded. Medium was replaced every 3–4 days. Two weeks after plating, cells were fixed and stained by crystal violet.

Anchorage-Independent Growth

Anchorage-independent growth was determined by assaying colony formation in soft agar. Cells (10^4) were suspended in 0.5 ml of growth medium containing blasticidin and 0.3% Seaplaque low-melting-temperature agarose (BMA, Rockland, ME) and plated in triplicates in a 6-well plate over a 1.5 ml layer of solidified 0.5% agarose/medium mixture. The cells were fed every 3 days by adding 100 μl of blasticidin-containing growth medium. Colonies were photographed at ×50 magnification after 2 weeks using a binocular microscope.

Northern Blot, In Situ Hybridization, and Cancer Profiling Arrays

Protocols for northern blot, in situ hybridization using the Soft Tissue Cancer tissue array (SO801, US Biomax), and detection of myocardin and vimentin using cancer profiling array II (Clontech) are provided in the Supplemental Data.

Analysis of Myocardin Promoter Methylation

Details of methylation-specific PCR and bisulfite sequencing are provided in the Supplemental Data.

Supplemental Data

The Supplemental Data include Supplemental Experimental Procedures and seven supplemental figures and can be found with this article online at http://www.cancercell.org/cgi/content/full/11/2/133/DC1/.

ACKNOWLEDGMENTS

The authors would like to thank Dr. Dina Ron for her helpful advice on in situ hybridization analysis. This research was supported by a Center of Excellence Grant from the Flight Attendant Medical Research Institute (FAMRI) and the Yad Abraham Center for Cancer Diagnosis and Therapy. V.R. is the incumbent of the Norman and Helen Asher Professorial Chair Cancer Research at the Weizmann Institute of Science.

Received: June 4, 2006
Revised: September 29, 2006
Accepted: November 28, 2006
Published: February 12, 2007

REFERENCES

Button, E., Shapland, C., and Lawson, D. (1995). Actin, its associated proteins and metastasis. Cell Motil. Cytoskeleton *30*, 247–251.

Chambers, R.C., Leoni, P., Kaminski, N., Laurent, G.J., and Heller, R.A. (2003). Global expression profiling of fibroblast responses to transforming growth factor-β1 reveals the induction of inhibitor of differentiation-1 and provides evidence of smooth muscle cell phenotypic switching. Am. J. Pathol. *162*, 533–546.

Dhanasekaran, S.M., Barrette, T.R., Ghosh, D., Shah, R., Varambally, S., Kurachi, K., Pienta, K.J., Rubin, M.A., and Chinnaiyan, A.M. (2001). Delineation of prognostic biomarkers in prostate cancer. Nature *412*, 822–826.

Du, K.L., Ip, H.S., Li, J., Chen, M., Dandre, F., Yu, W., Lu, M.M., Owens, G.K., and Parmacek, M.S. (2003). Myocardin is a critical serum response factor cofactor in the transcriptional program regulating smooth muscle cell differentiation. Mol. Cell. Biol. *23*, 2425–2437.

Halevy, O., Novitch, B.G., Spicer, D.B., Skapek, S.X., Rhee, J., Hannon, G.J., Beach, D., and Lassar, A.B. (1995). Correlation of terminal cell cycle arrest of skeletal muscle with induction of p21 by MyoD. Science *267*, 1018–1021.

Helman, L.J., and Meltzer, P. (2003). Mechanisms of sarcoma development. Nat. Rev. Cancer *3*, 685–694.

Horiuchi, A., Nikaido, T., Taniguchi, S., and Fujii, S. (1999). Possible role of calponin h1 as a tumor suppressor in human uterine leiomyosarcoma. J. Natl. Cancer Inst. *91*, 790–796.

Islam, A.H., Ehara, T., Kato, H., Hayama, M., and Nishizawa, O. (2004). Loss of calponin h1 in renal angiomyolipoma correlates with aggressive clinical behavior. Urology *64*, 468–473.

Kogan, I., Goldfinger, N., Milyavsky, M., Cohen, M., Shats, I., Dobler, G., Klocker, H., Wasylyk, B., Voller, M., Aalders, T., et al. (2006). hTERT-immortalized prostate epithelial and stromal-derived cells: An authentic in vitro model for differentiation and carcinogenesis. Cancer Res. *66*, 3531–3540.

Krimpenfort, P., Quon, K.C., Mooi, W.J., Loonstra, A., and Berns, A. (2001). Loss of p16Ink4a confers susceptibility to metastatic melanoma in mice. Nature *413*, 83–86.

Kumar, M.S., and Owens, G.K. (2003). Combinatorial control of smooth muscle-specific gene expression. Arterioscler. Thromb. Vasc. Biol. *23*, 737–747.

Lapointe, J., Li, C., Higgins, J.P., van de Rijn, M., Bair, E., Montgomery, K., Ferrari, M., Egevad, L., Rayford, W., Bergerheim, U., et al. (2004). Gene expression profiling identifies clinically relevant subtypes of prostate cancer. PNAS *101*, 811–816. Published online January 7, 2004. 10.1073/pnas.0304146101.

Leavitt, J., Gunning, P., Kedes, L., and Jariwalla, R. (1985). Smooth muscle alpha-action is a transformation-sensitive marker for mouse NIH 3T3 and Rat-2 cells. Nature *316*, 840–842.

Li, S., Wang, D.Z., Wang, Z., Richardson, J.A., and Olson, E.N. (2003). The serum response factor coactivator myocardin is required for vascular smooth muscle development. Proc. Natl. Acad. Sci. USA *100*, 9366–9370.

Ma, Z., Morris, S.W., Valentine, V., Li, M., Herbrick, J.A., Cui, X., Bouman, D., Li, Y., Mehta, P.K., Nizetic, D., et al. (2001). Fusion of two novel genes, RBM15 and MKL1, in the t(1;22)(p13;q13) of acute megakaryoblastic leukemia. Nat. Genet. *28*, 220–221.

MacKenzie, K.L., Franco, S., May, C., Sadelain, M., and Moore, M.A. (2000). Mass cultured human fibroblasts overexpressing hTERT encounter a growth crisis following an extended period of proliferation. Exp. Cell Res. *259*, 336–350.

Massague, J., Blain, S.W., and Lo, R.S. (2000). TGFβ signaling in growth control, cancer, and heritable disorders. Cell *103*, 295–309.

Meerson, A., Milyavsky, M., and Rotter, V. (2004). p53 mediates density-dependent growth arrest. FEBS Lett. *559*, 152–158.

Milyavsky, M., Shats, I., Erez, N., Tang, X., Senderovich, S., Meerson, A., Tabach, Y., Goldfinger, N., Ginsberg, D., Harris, C.C., et al. (2003). Prolonged culture of telomerase-immortalized human fibroblasts leads to a premalignant phenotype. Cancer Res. *63*, 7147–7157.

Milyavsky, M., Tabach, Y., Shats, I., Erez, N., Cohen, Y., Tang, X., Kalis, M., Kogan, I., Buganim, Y., Goldfinger, N., et al. (2005). Transcriptional programs following genetic alterations in p53, INK4A, and H-Ras genes along defined stages of malignant transformation. Cancer Res. *65*, 4530–4543.

Novitch, B.G., Mulligan, G.J., Jacks, T., and Lassar, A.B. (1996). Skeletal muscle cells lacking the retinoblastoma protein display defects in muscle gene expression and accumulate in S and G2 phases of the cell cycle. J. Cell Biol. *135*, 441–456.

Papadimou, E., Menard, C., Grey, C., and Puceat, M. (2005). Interplay between the retinoblastoma protein and LEK1 specifies stem cells toward the cardiac lineage. EMBO J. *24*, 1750–1761.

Pipes, G.C., Creemers, E.E., and Olson, E.N. (2006). The myocardin family of transcriptional coactivators: Versatile regulators of cell growth, migration, and myogenesis. Genes Dev. *20*, 1545–1556.

Rhodes, D.R., Yu, J., Shanker, K., Deshpande, N., Varambally, R., Ghosh, D., Barrette, T., Pandey, A., and Chinnaiyan, A.M. (2004). Large-scale meta-analysis of cancer microarray data identifies common transcriptional profiles of neoplastic transformation and progression. Proc. Natl. Acad. Sci. USA *101*, 9309–9314.

Serini, G., and Gabbiani, G. (1999). Mechanisms of myofibroblast activity and phenotypic modulation. Exp. Cell Res. *250*, 273–283.

Sharpless, N.E., Bardeesy, N., Lee, K.H., Carrasco, D., Castrillon, D.H., Aguirre, A.J., Wu, E.A., Horner, J.W., and DePinho, R.A. (2001). Loss of p16Ink4a with retention of p19Arf predisposes mice to tumorigenesis. Nature *413*, 86–91.

Taylor, L.M., James, A., Schuller, C.E., Brce, J., Lock, R.B., and Mackenzie, K.L. (2004). Inactivation of p16INK4a, with retention of pRB and p53/p21cip1 function, in human MRC5 fibroblasts that overcome a telomere-independent crisis during immortalization. J. Biol. Chem. *279*, 43634–43645.

Thomas, D.M., Carty, S.A., Piscopo, D.M., Lee, J.S., Wang, W.F., Forrester, W.C., and Hinds, P.W. (2001). The retinoblastoma protein acts as a transcriptional coactivator required for osteogenic differentiation. Mol. Cell *8*, 303–316.

Wang, D., Chang, P.S., Wang, Z., Sutherland, L., Richardson, J.A., Small, E., Krieg, P.A., and Olson, E.N. (2001). Activation of cardiac gene expression by myocardin, a transcriptional cofactor for serum response factor. Cell *105*, 851–862.

Wieser, R.J., Faust, D., Dietrich, C., and Oesch, F. (1999). p16INK4 mediates contact-inhibition of growth. Oncogene *18*, 277–281.

Yamamura, H., Yoshikawa, H., Tatsuta, M., Akedo, H., and Takahashi, K. (1998). Expression of the smooth muscle calponin gene in human osteosarcoma and its possible association with prognosis. Int. J. Cancer *79*, 245–250.

Zhang, H.S., Postigo, A.A., and Dean, D.C. (1999). Active transcriptional repression by the Rb-E2F complex mediates G1 arrest triggered by p16INK4a, TGFβ, and contact inhibition. Cell *97*, 53–61.

Zou, T.T., Selaru, F.M., Xu, Y., Shustova, V., Yin, J., Mori, Y., Shibata, D., Sato, F., Wang, S., Olaru, A., et al. (2002). Application of cDNA microarrays to generate a molecular taxonomy capable of distinguishing between colon cancer and normal colon. Oncogene *21*, 4855–4862.